This article has been accepted for publication in a future issue of this journal, but has not been fully edited. Content may change prior to final publication. Citation information: DOI 10.1109/TMECH.2016.2527240, IEEE/ASME Transactions on Mechatronics

A simplified upper body model to improve the external validity of wheelchair simulators

Félix Chénier[1,2,3], Dany H. Gagnon[1,3], Martine Blouin[4,5] and Rachid Aissaoui[1,4,5]

***Abstract*—During overground wheelchair propulsion, upper body movement causes intra-cycle velocity variations that are neglected by current wheelchair simulators. This could affect the external validity of wheelchair propulsion on simulators. In this work, we investigated ways to incorporate these dynamics into the dynamic model (DM) reproduced by wheelchair simulators. We aimed to maximize the DM accuracy and minimize the number of required inputs. First, two DMs were presented: Model RL represented propulsion on a typical roller-based wheelchair simulator and model UB (upper body) represented overground propulsion, modelling the upper body as 5 rigid bodies. Then, three new DMs were presented: Model TR (trunk), model UA (upper arm) and model FA (forearm); these models simplified model UB by estimating the upper body kinematics based on the acceleration of only one segment. For all DMs, wheelchair velocity prediction was tested overground at a self-selected velocity among 19 experienced manual wheelchair users with a spinal cord injury. Upper body kinematics was reconstructed based on personalized kinematic patterns recorded on a wheelchair simulator. Models UB and UA were the most accurate: they reduced the root-mean-square intra-cycle velocity prediction error from 0.044 m/s (RL) to 0.026 m/s (UB) and 0.024 m/s (UA), and reduced the velocity peak time prediction error from -27.7 % (RL) to 1.7 % (UB) and -7.3 % (UA). Implementing model UA instead of model RL on a wheelchair simulator may improve the external validity of wheelchair propulsion on a simulator.**

***Index Terms*—Biomechanics, Dynamics, Kinematics, Biomedical Engineering, Motion analysis, Rehabilitation, Wheelchairs.**

I. Introduction

Wheelchair simulators are devices that simulate real wheelchair propulsion conditions in a stationary environment. They usually consist of a fixed wheelchair with both rear wheels placed over two inertial rollers. [1]. A wheelchair simulator provides controlled wheeling conditions, allows for the use of stationary instruments which would not be possible in an ambulatory setting, and allows continuous data acquisition over an extended period of time, such as with endurance training in a limited space. Recently, a wheelchair simulator has been used for the first time to optimize wheelchair users' propulsion techniques using haptic biofeedback [2].

To generalize the study results obtained using a simulator to overground propulsion and ensure that training on a simulator is transferable to overground propulsion, the simulator must reproduce wheelchair propulsion in a reliable and valid manner. Unfortunately, current wheelchair simulators typically model the wheelchair/user system as a single inertial body driven by two opposite forces: a propulsion force resulting from the propulsive moments applied on the handrims by the user and a constant rolling resistance force. The dynamics of the upper body segments, which are known to generate intra-cycle velocity variations [3–5], are neglected by such a simple model. More precisely, it was observed that the wheelchair accelerates not only during the push phase but also during the recovery phase when no propulsion moments are applied [3–5]. This is inherent to the pushing action that requires a forward acceleration of the upper body, which contributes to a deceleration of the wheelchair. In contrast, the backward acceleration of the upper body after the push generates an acceleration of the wheelchair during the recovery phase.

Given recent technology advancements, today's wheelchair simulators can now reproduce a virtually dynamic model (DM) [6, 7]. Therefore, the external validity of such simulators is currently contingent on the DM they simulate. A DM of the wheelchair/user system is a set of equations that predicts the velocity of a wheelchair based on dynamic input from the user and his/her environment. Crichlow [7] recently presented a simulator-oriented wheelchair/user DM that includes the upper body movement dynamics. This DM uses a motion capture system to obtain upper body positions in real time. While this is a relevant approach, it requires an expensive real-time motion capture system, increases the setup time before a user can propel on the simulator and requires rehabilitation engineering and technical assistance.

In this paper, we first presented the DM of a roller ergometer (model RL) and the DM of the wheelchair/user system, the latter being based on the anteroposterior acceleration of five upper-body segments (model UB). Then, we proposed three new simplified DMs that limit the required input information to the anteroposterior of one segment: trunk (model TR), upper arm (model UA) and forearm (model FA). The main aim of this work was to improve the velocity prediction accuracy of the DM while minimizing the number of required kinematic inputs.

II. Methodology

A. Participants

Propulsion data from a previous study on wheelchair propulsion was used in this work [2]. Nineteen (19) participants were included in our study, contrary to 18 in the previous study

[1] Centre for interdisciplinary research in rehabilitation of Greater Montreal. [2] Dept. of Physical Activity Science, Université du Québec à Montréal. [3] Dept. of Medicine, University of Montreal. [4] Laboratoire de recherche en Imagerie et Orthopédie (LIO), Centre de recherche du Centre hospitalier de l'Université de Montréal (CRCHUM). [5] Département de génie de la production automatisée, École de technologie supérieure, Montréal.

Corresponding author: Félix Chénier. Email: felix@felixchenier.com. Phone: +1 (514) 987-3000 ext.5553. Address: Université du Québec à Montréal, Office SB-4455, 141 Président-Kennedy, Montréal QC, H2X 1Y4

1083-4435 (c) 2015 IEEE. Personal use is permitted, but republication/redistribution requires IEEE permission. See http://www.ieee.org/publications_standards/publications/rights/index.html for more information.

This article has been accepted for publication in a future issue of this journal, but has not been fully edited. Content may change prior to final publication. Citation information: DOI 10.1109/TMECH.2016.2527240, IEEE/ASME Transactions on Mechatronics

where one participant did not complete the required additional data acquisition session on the simulator. Participants were diagnosed with a complete or incomplete spinal cord injury (AIS A, B or C) between C7 and L1 that was sustained at least three months previously. They used a wheelchair as their primary means of mobility and were able to transfer independently. The project was approved by the research ethics committees of the École de technologie supérieure (ÉTS) and the Centre for Interdisciplinary Research in Rehabilitation of Greater Montreal (CRIR). Participants gave their informed consent to use the collected anonymized data for related studies requiring secondary analyses. Data were collected during a single visit.

B. Materials

For the acquisitions overground, the participants' own wheelchairs were equipped with two 24-inch instrumented wheels (SmartWheel, Out-front Corp., Mesa, AZ, USA). The wheelchair and instrumented wheels were weighed using an adapted scale (Health O Meter, Pelstar LCC, McCook, IL, USA). For the acquisitions on the simulator, the simulator described in Chénier et al. [8] was used to measure participants' upper body kinematics. Reflective markers were installed on participants' xiphoid process, acromions, lateral elbow epicondyles and ulnar styloids (Fig. 1). Marker positions were recorded using six cameras (Vicon Motion Systems Ltd., Oxford, UK) at a sampling rate of 120 Hz. The simulated mass was adjusted to the total wheelchair/user mass m, and the simulated rolling resistance was adjusted to $F_{\text{roll}} = mg\mu$, where $g = 9.81$ m/s^2 and $\mu = 0.0138$ N/N [8].

C. Experimental tasks

Participants propelled their wheelchairs on a flat tiled corridor over a distance of 20 meters at a self-selected velocity. Forces and moments applied on the wheels as well as wheel angles were recorded bilaterally at a sampling rate of 240 Hz. Upper body kinematics was not measured during overground propulsion. However, since intra-subject propulsion kinematics is very repeatable, especially for the upper arms and forearms [9], a personalized kinematic pattern was used to reconstruct overground propulsion kinematics. This implicit assumption that the kinematics recorded on a simulator is transferable to overground propulsion will be discussed later. To generate this personalized kinematics pattern, participants propelled at a self-selected velocity on the simulator for 30 seconds. Participants were not given any velocity feedback, therefore velocity on the simulator was measured but not controlled.

D. Dynamic models

The five DMs that were tested are described in the following paragraphs. For all models, the vertical movement of the system's centre of mass (COM) was not considered and the effect of the COM's fore-and-aft displacement on the rolling resistance was neglected. Based on estimations by Sauret et al. [3], the rolling resistance varies in a range of ±7 % during a propulsion cycle. In our setup where the average rolling resistance was about 14 N, this limits the variation to ± 1 N, which is much smaller than our observed resultant propulsive forces of 50 N to 100 N (Fig 3).

1) Model RL (rollers): This model predicts the virtual wheelchair velocity based on the propulsive moments applied on the wheels by the user, assuming the wheels do not slip. This is a unidimensional model where rollers provide a moment of rolling resistance M_{roll} and a moment of inertia J_{roller}. Ideally, M_{roll} and J_{roller} are matched to the actual rolling resistance F_{roll} and mass m of the wheelchair/user system so that the simulator dynamics follows (1), which describes a simplified wheelchair/user dynamic system [8, 10]:

$$F_{\text{prop}} - F_{\text{roll}} = m\ddot{x}_0 \tag{1}$$

where the total propulsive force F_{prop} is expressed as:

$$F_{\text{prop}} = \frac{1}{r_R}(M_L + M_R) \tag{2}$$

and where $\ddot{x}_0$ is the acceleration of the wheelchair/user system origin (reference frame 0 located at the middle of the rear wheel axis) in the global reference frame, r_R is the rear wheels radius, and M_L and M_R are the propulsive moments applied by the user on the rear wheels. Wheelchair velocity is predicted by time-integrating (1):

$$\hat{\dot{x}}_{0(\text{RL})} = (1/m) \int \left(F_{\text{prop}} - F_{\text{roll}}\right) dt \tag{3}$$

2) Model UB (upper body): This model predicts the wheelchair velocity based on the propulsive moments and the user's upper body kinematics. The wheelchair/user system is divided into six segments: segment 0, which combines the wheelchair and lower body, and segments 1 to 5 as illustrated in Fig. 1. This model can be expressed as:

$$F_{\text{prop}} - F_{\text{roll}} = \sum_{i=0}^{5} m_i \ddot{x}_i \tag{4}$$

where m_i is the mass of segment i and $\ddot{x}_i$ is its anteroposterior acceleration in the global reference frame. By expressing the accelerations of the upper body segments ($\ddot{x}_1$ to $\ddot{x}_5$) relative to the wheelchair (reference frame 0), we obtain:

$$F_{\text{prop}} - F_{\text{roll}} = m\ddot{x}_0 + \sum_{i=1}^{5}(m_i \, {}^0\ddot{x}_i) \tag{5}$$

where ${}^0\ddot{x}_i$ is the acceleration of segment i relative to reference frame 0. Based on (5), wheelchair velocity is predicted as a function of the propulsive forces F_{prop} and the upper body segments' anteroposterior acceleration ${}^0\ddot{x}_i$:

$$\hat{\dot{x}}_{0(\text{UB})} = (1/m) \int \left(F_{\text{prop}} - F_{\text{roll}} - \sum_{i=1}^{5}(m_i \, {}^0\ddot{x}_i)\right) dt \tag{6}$$

3) Model TR (trunk): This model simplifies model UB to reduce the number of required kinetic inputs. In our data, although the trunk movement was nearly null (Fig. 3), it is still the heaviest segment of the upper body. Therefore, model TR is a reduction of model UB where only the trunk segment is included:

$$F_{\text{prop}} - F_{\text{roll}} = m\ddot{x}_0 + m_5 \, {}^0\ddot{x}_5 \tag{7}$$

1083-4435 (c) 2015 IEEE. Personal use is permitted, but republication/redistribution requires IEEE permission. See http://www.ieee.org/publications_standards/publications/rights/index.html for more information.

Based on (7), wheelchair velocity is predicted as a function of the propulsive forces F_{prop} and the trunk's anteroposterior acceleration ${}^0\ddot{x}_5$:

$$\hat{\dot{x}}_{0(\text{TR})} = (1/m) \int \left(F_{\text{prop}} - F_{\text{roll}} - m_5 \, {}^0\ddot{x}_5 \right) dt \tag{8}$$

4) Model UA (upper arm): This model also simplifies model UB to reduce the required kinematic input, this time to the upper arm acceleration. To this effect, we add simplifying assumptions to model UB to express ${}^0\ddot{x}_2$ to ${}^0\ddot{x}_5$ as a function of ${}^0\ddot{x}_1$. Four additional constraints are required.

Assumption 1: Propulsion movement is symmetrical. This adds the following two constraints: ${}^0\ddot{x}_1 = {}^0\ddot{x}_3$, ${}^0\ddot{x}_2 = {}^0\ddot{x}_4$.

Assumption 2: The trunk dynamics is negligible at a self-selected velocity. This assumption, which will be discussed later based on simulation results of model TR, allows us to introduce the following constraint: ${}^0\ddot{x}_5 = 0$.

The last required constraint relates forearm acceleration ${}^0\ddot{x}_2$ to upper arm acceleration ${}^0\ddot{x}_1$. We know that ${}^0\ddot{x}_2$ is effectively a function of ${}^0\ddot{x}_1$, but also of the flexion angle and flexion acceleration of the elbow. To express ${}^0\ddot{x}_2$ as a function of ${}^0\ddot{x}_1$ only, we introduce the following assumption:

Assumption 3: Forearm orientation is constant (Fig. 2). This implies that the anteroposterior acceleration of the forearm COM is equal to the anteroposterior acceleration of the elbow. Therefore:

$${}^0\ddot{x}_2 = (l_1/d_1) \, {}^0\ddot{x}_1 \tag{9}$$

where l_1 is the length of the upper arm, and d_1 is the distance of the upper arm COM from the acromion. Figure 2 illustrates assumptions 2 and 3 based on real kinematic data from a typical participant. We observe that constraining the shoulder to a fixed point (assumption 2) has little impact on the trajectory of upper arm COM. Moreover, constraining the forearm to a constant angle (assumption 3) does have an impact on the trajectory of forearm COM, but this impact is much less important on the anteroposterior axis than on the vertical axis. As a matter of fact, the Pearson's coefficient of correlation between the real and estimated anteroposterior position of the left forearm COM following assumption 3 was of 0.979 ± 0.014 for the 19 participants of this work. According to assumptions 1 to 3, (5) resolves to:

$$F_{\text{prop}} - F_{\text{roll}} = m\ddot{x}_0 + 2\left(m_1 + \frac{l_1 m_2}{d_1}\right) {}^0\ddot{x}_1 \tag{10}$$

Based on (10), wheelchair velocity is predicted as a function of the propulsive forces F_{prop} and upper arm acceleration ${}^0\ddot{x}_1$:

$$\hat{\dot{x}}_{0(\text{UA})} = (1/m) \int \left(F_{\text{prop}} - F_{\text{roll}} - 2\left(m_1 + \frac{l_1 m_2}{d_1}\right) {}^0\ddot{x}_1 \right) dt \tag{11}$$

5) Model FA (forearm): As for model UA, model FA predicts wheelchair velocity based on the propulsive moments and anteroposterior acceleration of one segment: the forearm. Thus, the same assumptions 1 to 3 are made and (5) resolves to:

$$F_{\text{prop}} - F_{\text{roll}} = m\ddot{x}_0 + 2\left(m_2 + \frac{d_1 m_1}{l_1}\right) {}^0\ddot{x}_2 \tag{12}$$

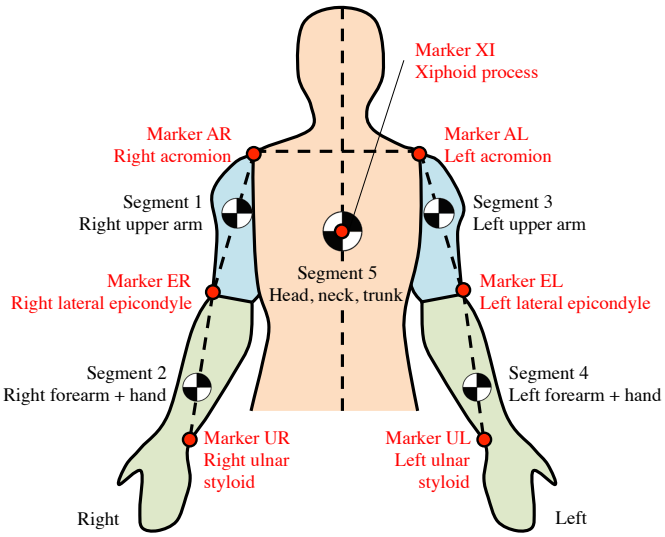

Figure 1: Five-segment decomposition of the upper body: anatomic placement of the seven kinematic markers (anterior view)

Therefore, wheelchair velocity is predicted as a function of the propulsive forces F_{prop} and forearm acceleration $\ddot{x}_2$:

$$\hat{\dot{x}}_{0(\text{FA})} = (1/m) \int \left(F_{\text{prop}} - F_{\text{roll}} - 2\left(m_2 + \frac{d_1 m_1}{l_1}\right) {}^0\ddot{x}_2 \right) dt \tag{13}$$

E. Data processing

The predicted velocity was calculated for the five models following these steps:

1) Reconstruction of propulsion kinematics: The personalized upper body kinematics pattern recorded on the simulator for each participant was defined as the position of each segment's COM during an average propulsion cycle. The anteroposterior position ${}^0x_i$ of COM of each segment relative to the wheelchair origin was estimated from the position of the markers based on anthropometric tables:

$$\begin{aligned}
{}^0x_1 &= d_1/l_1 (x_{\text{ER}} - x_{\text{AR}}) + x_{\text{AR}} && (14)\\
{}^0x_2 &= d_2/l_2 (x_{\text{UR}} - x_{\text{ER}}) + x_{\text{ER}} && (15)\\
{}^0x_3 &= d_1/l_1 (x_{\text{EL}} - x_{\text{AL}}) + x_{\text{AL}} && (16)\\
{}^0x_4 &= d_2/l_2 (x_{\text{UL}} - x_{\text{EL}}) + x_{\text{EL}} && (17)\\
{}^0x_5 &= x_{\text{XI}} && (18)
\end{aligned}$$

where $d_1/l_1 = 0.436$, $d_2/l_2 = 0.682$ [11], l_2 is the length of the forearm and d_2 is the distance of the forearm+hand COM from the elbow.

Push detection was performed using a double threshold on the sum of the vectorial forces applied on both wheels by the user. Values of 20 N (onset) and 10 N (offset) were selected experimentally to maximize detected push length while minimizing false detections. The 10 most repeatable pushes were selected individually by minimizing the variance of the waveforms of the propulsive moments applied on the right wheel, following the cycle selection method proposed

This article has been accepted for publication in a future issue of this journal, but has not been fully edited. Content may change prior to final publication. Citation information: DOI 10.1109/TMECH.2016.2527240, IEEE/ASME Transactions on Mechatronics

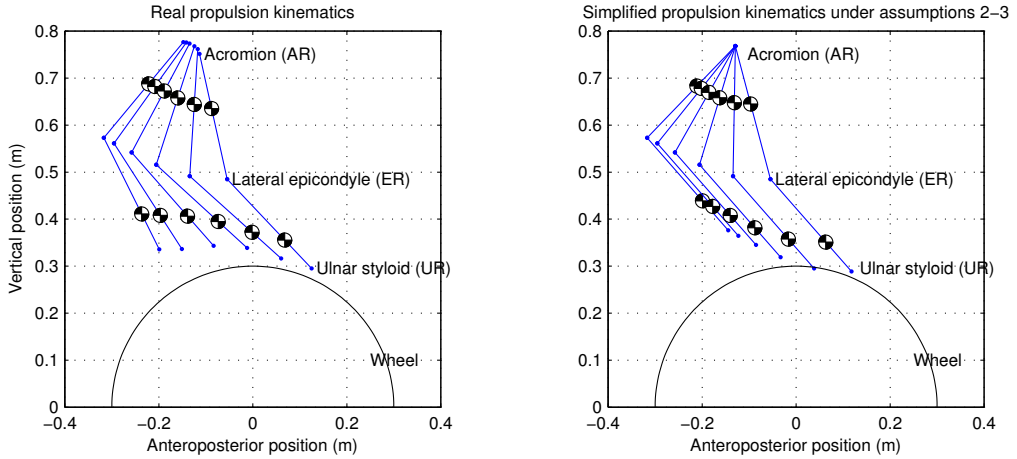

Figure 2: Illustration of assumptions 2 and 3 in the sagittal plane, for propulsion on a simulator at self-selected velocity.

by Kadaba et al. [12]. The personalized kinematic pattern was obtained by averaging x_1 to x_5 curves over these 10 pushes.

The upper body kinematics curves were then reconstructed for overground propulsion by time scaling ${}^0x_1$ to ${}^0x_5$ for each propulsion cycle. All signals were resampled on a common time vector at 240 Hz (the sampling frequency of the instrumented wheels). Figure 3 shows the reconstructed kinematics for a typical participant.

2) Segment mass and acceleration: Segment mass was estimated based on anthropometric tables [11]:

$$m_1 = m_3 = 0.028 \times m_{\text{participant}} \quad (19)$$

$$m_2 = m_4 = 0.022 \times m_{\text{participant}} \quad (20)$$

$$m_5 = 0.578 \times m_{\text{participant}} \quad (21)$$

Relative segment accelerations ${}^0\ddot{x}_1$ to ${}^0\ddot{x}_5$ were obtained by filtering the reconstructed propulsion kinematics ${}^0x_1$ to ${}^0x_5$ using a double-derivative Savitsky-Golay filter. Savitsky-Golay filters do not have a phase lag, are very flat in their bandwidth and are well suited to estimating n$^{\text{th}}$ derivatives of noisy signals [13]. To maintain a bandwidth of 6 Hz, a second-order filter with a window length of 0.32 seconds was selected [14].

3) Wheelchair velocity and power output: The measured velocity was obtained by filtering the encoded angular position of each rear wheel using a first-derivative Savitsky-Golay filter with the same order and window length. The predicted velocity for each model was obtained using equations (3), (6), (8), (11) and (13). The measured and predicted power output was obtained by multiplying the measured and predicted wheelchair velocity by the total propulsive force F_{prop}.

4) Outcome variables: For both variables (velocity, power output), the following outcome variables were calculated:

- The span (difference between minimum and maximum) during the complete propulsion cycle for velocity, or during the push for power output;
- The time at which the peak value occured, expressed as a percentage of the complete propulsion cycle for velocity, or of the push for power output;
- For the predicted variables, the root-mean-square (RMS) prediction error between the measured curve and the predicted curve (ε_{vel} for velocity, ε_{PO} for power output).

Every participants needed to perform at least 10 pushes to complete the 20-meter overground path. Push cycles 1 to 4 and the last push were considered as transitional (startup and coast down). Therefore, outcome measures were calculated on push cycles 5 to 9, then averaged over these five cycles.

5) Statistical analysis: The predicted variables (velocity span, peak time, power output span, peak time) were compared to the measured ones using an analysis of variance (ANOVA) with repeated measures. The RMS prediction errors ($\varepsilon_{\text{vel}}, \varepsilon_{\text{po}}$) were compared between models with an ANOVA with repeated measures. When a significant difference was found, a Tukey-Kramer post-hoc test was performed to compare the models' predictions independently. A significance level of $\alpha = 0.05$ was selected for all tests.

6) Sensitivity analysis: Models TR, UB, UA and FA are dependent on the mass of the segments, which is obtained via anthropometric tables. To observe the sensitivity of the velocity prediction to these segments masses, we performed a sensitivity analysis of ε_{vel} for independent variations of trunk mass, upper arm mass, forearm mass and total upper body mass in intervals of $[-20\%, -10\%, 0\%, +10\%, +20\%]$.

III. Results

A. Velocity

The participants chose a self-selected velocity of 1.47 ± 0.37 m/s overground, and of 1.14 ± 0.21 m/s on the simulator. The difference between both velocities were significant (paired t-test, $p < 0.001$). Table I shows the measured and predicted velocity overground. For all conditions, the velocity varied by 0.10 to 0.16 m/s during a propulsion cycle. When comparing the models' predictions with measured data, we found statistically significant differences of both span and peak time, the latter being the main difference between models. Models RL and TR both significantly underestimated the velocity peak time while model UA also underestimated the velocity peak time but at a lesser extent. Models UB, UA and FA had significantly lower velocity RMS errors than model RL. Based on these results, the best model in terms of velocity prediction is UB, followed by UA and FA, then by RL and TR.

1083-4435 (c) 2015 IEEE. Personal use is permitted, but republication/redistribution requires IEEE permission. See http://www.ieee.org/publications_standards/publications/rights/index.html for more information.

This article has been accepted for publication in a future issue of this journal, but has not been fully edited. Content may change prior to final publication. Citation information: DOI 10.1109/TMECH.2016.2527240, IEEE/ASME Transactions on Mechatronics

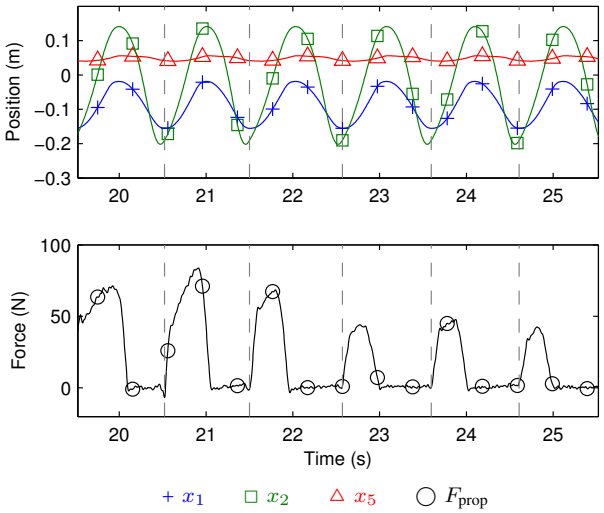

Figure 3: Reconstruction of upper-body kinematics for over-ground propulsion at self-selected velocity, by time-scaling x_1 to x_5 over each push. Only right upper arm (+), right forearm (□) and trunk (△) COM positions are shown. Pushes start when the propulsive force F_{prop} (○) reaches 20 N.

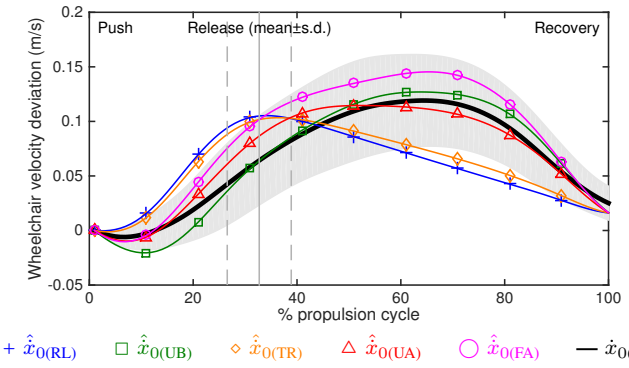

Figure 4: Average velocity profile for all participants. The grey shading represents the standard deviation of the measured velocity deviation.

Figure 4 shows the velocity profile averaged over all participants. As the self-selected velocity was different between participants, the figure is presented as a deviation from the initial velocity at the beginning of the propulsion cycle. The underestimation of velocity peak time is clearly visible for models RL and TR, whereas models UB, UA and FA follow a profile more similar to the measured velocity. A sample of an accurate velocity prediction by models UB, UA and FA is shown in Figure 5: in this case, models UB, UA and FA were all more accurate than the models RL and TR in predicting wheelchair velocity. On the other hand, a sample of an inaccurate velocity prediction by every models is shown in Figure 6.

The results from the sensitivity analysis are shown in Fig. 7. The maximal sensitivity was observed with models UB and FA, where a variation of -20% to +20% of the total upper body mass caused a variation of 0.01 m/s RMS.

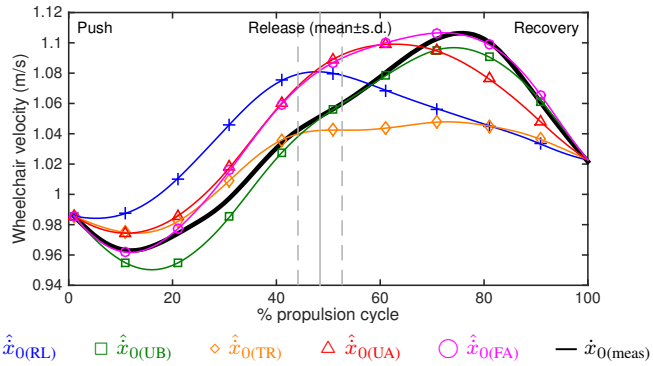

Figure 5: Good agreement between measured and predicted velocities

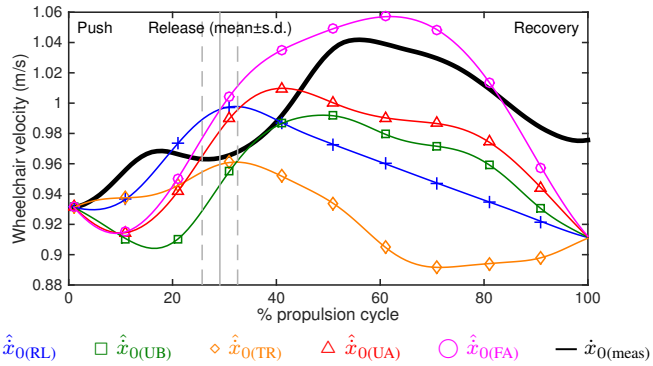

Figure 6: Poor agreement between measured and predicted velocities

Table I: Measured and predicted velocity

		Av	SD	Diff with meas Av	Diff with meas SD
Measured	Span (m/s)	0.135	0.026		
	Peak time (%)	61.2	5.7		
RL	Span (m/s)	0.118	0.026	-0.016	0.035
	Peak time (%)	33.5	5.7	**-27.7**	7.6
	RMS diff (m/s)	0.044	0.013		
UB	Span (m/s)	0.160	0.045	**0.025** †	0.036
	Peak time (%)	62.9	8.8	1.7 †	6.7
	RMS diff (m/s)	0.026 †	0.012		
TR	Span (m/s)	0.098	0.035	**-0.037** †	0.035
	Peak time (%)	45.2	18.8	**-16.1** †	15.0
	RMS diff (m/s)	0.039	0.020		
UA	Span (m/s)	0.137	0.038	0.002 †	0.031
	Peak time (%)	53.9	12.4	-7.3 †	9.6
	RMS diff (m/s)	0.024 †	0.010		
FA	Span (m/s)	0.164	0.034	**0.029** †	0.030
	Peak time (%)	65.3	5.7	4.1 †	6.0
	RMS diff (m/s)	0.031 †	0.016		

Bold: Statistically different from the measured value
† : Statistically different from Model RL

1083-4435 (c) 2015 IEEE. Personal use is permitted, but republication/redistribution requires IEEE permission. See http://www.ieee.org/publications_standards/publications/rights/index.html for more information.

This article has been accepted for publication in a future issue of this journal, but has not been fully edited. Content may change prior to final publication. Citation information: DOI 10.1109/TMECH.2016.2527240, IEEE/ASME Transactions on Mechatronics

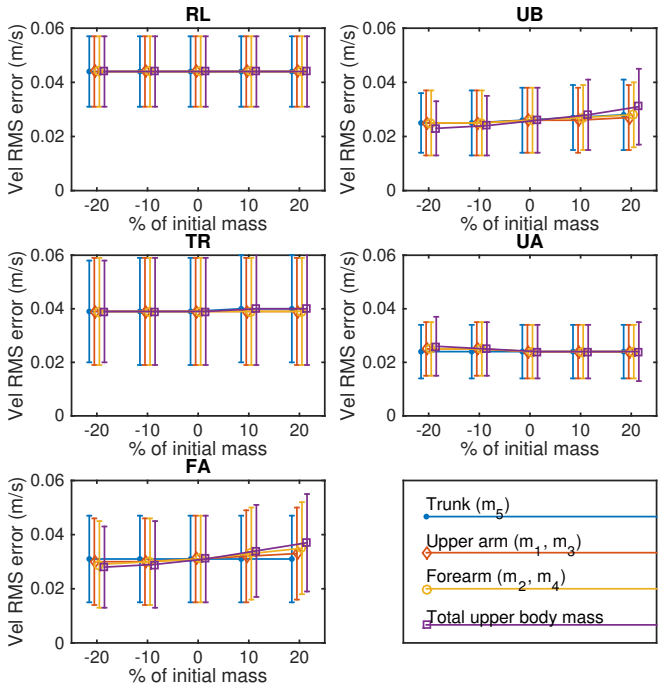

Figure 7: Sensitivity analysis: effect of the segments mass on ε_{vel}

Table II: Measured and predicted power output

				Diff with meas	
		Av	SD	Av	SD
Measured	Span (W)	100.25	45.39		
	Peak time (%)	18.8	4.7		
RL	Span (W)	103.30	45.39	**3.06**	1.92
	Peak time (%)	18.9	4.7	0.1	0.2
	RMS diff (W)	1.97	1.12		
UB	Span (W)	99.19	44.09	**-1.06** †	1.52
	Peak time (%)	18.9	4.7	0.1	0.2
	RMS diff (W)	0.96 †	0.61		
TR	Span (W)	101.31	44.68	**1.06** †	1.64
	Peak time (%)	18.9	4.7	0.1	0.2
	RMS diff (W)	0.96 †	0.71		
UA	Span (W)	100.89	44.84	0.65 †	1.48
	Peak time (%)	18.9	4.8	0.1	0.3
	RMS diff (W)	0.95 †	0.63		
FA	Span (W)	101.44	44.81	**1.19** †	1.55
	Peak time (%)	19.0	4.9	0.2	0.4
	RMS diff (W)	1.22 †	0.79		

Bold: Statistically different from the measured value
† : Statistically different from Model RL

B. Power output

Table II shows the measured and predicted power output variables. For all conditions (measured and predicted), the power output span varied from 99 to 103 W during a push. Statistically significant but small differences were observed between measured and predicted values for all models except UA. The peak time was well predicted by every model. Although no statistically significant difference in RMS prediction error was found between models, model RL had the highest error (3.06 W), followed by model FA (1.19 W) and then by the other models (about 1.0 W).

IV. Discussion

This study produced three key results: 1) including personalized upper body kinematics in the wheelchair/user system dynamic model (model UB) improved the velocity prediction compared to the model RL; 2) limiting the required kinematic information to the anteroposterior acceleration of one upper-arm (model UA) or one forearm (FA) still improved the velocity prediction compared to the model RL; and 3) limiting the required kinematic information to the trunk acceleration did not improve the velocity prediction compared to model RL. These three findings will be discussed in the following section.

A. Velocity

Model RL is a single inertial body. It can therefore only accelerate during the push phase because no forces are applied by the user during recovery. This was observed on '+' curves in Figures 4 to 6. However, we also observed that the real velocity does not reach its maximum at the end of the push phase but during the recovery phase instead. As mentioned in the introduction, this result is consistent with the existing literature [3–5], and is mainly due to the forward and backward acceleration of the upper body that is necessary to push the rear wheels. In contrast to model RL, model UB includes the upper body movement, which does result in a better prediction of wheelchair velocity, with half the RMS prediction error and an accurate velocity peak time.

The second objective of this investigation was to minimize the kinematic information required to incorporate upper body dynamics into a wheelchair/user DM. New models TR, UA and FA were approximations of model UB, based on the anteroposterior acceleration of only one segment. Although the trunk has the greatest mass compared to the arms, model TR was not better than model RL to predict the intra-cycle wheelchair velocity variation. Whereas models TR and RL globally have a similar velocity prediction in Figure 4, we observe that both models may produce very different results for individual participants (Figures 5 and 6). We also observe in Table I that model TR has the highest standard deviation for ε_{vel}, which suggests that the motion of the trunk may be erratic and variable between users and propulsion conditions. Although it does not confirm assumption 2 that the trunk dynamics is negligible at a self-selected velocity, it however indicates that the trunk motion could not be used as a reliable input to improve the DM of the wheelchair/user system.

The new models UA and FA were based on the assumption that the trunk does not move. Although this assumption could not be demonstrated, models UA and FA did reduce ε_{vel} significantly compared to the RL model. The predicted velocity peak time was also much more accurate with models UA and FA than with model RL. Model UA had the lowest RMS error ε_{vel} and a better predicted velocity span than model FA. Additionally, it had a lower standard deviation for ε_{vel}, which suggests that velocity prediction is more repeatable based on the motion of the upper arm than on the motion of the forearm. For these reasons, it appears that model UA

1083-4435 (c) 2015 IEEE. Personal use is permitted, but republication/redistribution requires IEEE permission. See http://www.ieee.org/publications_standards/publications/rights/index.html for more information.

This article has been accepted for publication in a future issue of this journal, but has not been fully edited. Content may change prior to final publication. Citation information: DOI 10.1109/TMECH.2016.2527240, IEEE/ASME Transactions on Mechatronics

should be selected over model FA when estimating upper body movement dynamics based on only one segment.

The sensitivity analysis (Fig. 7) showed that all models are almost insensitive to variations of segments mass. This was obviously expected for model RL, which is independent of upper body mass. The generalization of this insensitivity to the other models is advantageous because it means that the models will behave similarly regardless of the mass distribution of the user. This is critical for wheelchair propulsion, where able-bodied persons (on which the anthropometric tables are based) have a lower centre of mass than wheelchair users.

B. Power output

We observed in Table II that the power output was very similar between models. In our analysis, we assumed that the same force was applied as the input of every model, therefore, it is not surprising that the power output, which is the product of the force by the velocity, is similar between models. In reality, in any haptic relation between a user and an interface, the relation between force and velocity is not unidirectional: it is highly probable that the user would adapt his/her propulsion force pattern to the different presented DMs. Power output estimated in this work should therefore be taken with caution as it is expected to vary more between models in real life.

C. Limitations of the study

In this work, data acquisition was overground with experienced paraplegic wheelchair users, who are known to present different propulsion kinematics than able-bodied persons [15]. This makes it possible to generalize these results to the targeted population. In our opinion, the main limitation of this work is the overground reconstruction of upper body kinematics, based on propulsion data acquired on a simulator. This limitation was however necessary to allow models UB, TR, UA and FA to be tested in real overground conditions: a motion capture system was unavailable due to its restricted acquisition volume. The participants did change their self-selected velocity between overground and simulator propulsion. As upper body kinematics is known to change as a function of velocity [16, 17], then the participants may also have changed their kinematics between both conditions, which could be the main cause of discrepancies between measured and predicted velocities by model UB. Kinematics acquisition on a treadmill instead of on a roller-based simulator may have resulted in more realistic propulsion conditions since the dynamic effect of the upper-body movement may be reproduced. This however still needs to be verified, as Stephens and Engsberg [18] observed that persons with tetraplegia changed their kinematics either from overground to rollers or from overground to treadmill. Future work on the impact of velocity on upper body kinematics and on the repeatability of the upper body kinematics between overground and simulator propulsion is ongoing.

D. Relevance

Model UA was the most accurate among the simplified models TR, UA and FA. This result is highly relevant because it suggests that only the anteroposterior acceleration of one upper arm is required to estimate the intra-cycle velocity variation at a self-selected velocity. This acceleration may be estimated in real time using a simple inertial unit strapped onto the user's arm. An accelerometer is much cheaper than a real-time motion capture system; moreover, as it produces a single analog signal, it is easier than a motion capture system to interface with a wheelchair simulator. Future work in this area is being considered.

The relevance of velocity variation during the recovery phase could be overlooked: it is true that the user could not feel the wheels' velocity when his/her hands are not in contact with the handrims. However, if a visual flow is presented to the user, then the predicted wheelchair velocity during recovery becomes much important because the user now has visual velocity information even when he/she does not touch the wheels.

V. Conclusion

In this investigation, we evaluated the accuracy of five dynamic models (DM) of the wheelchair/user system in predicting overground wheelchair velocity. Our aim was to both maximize the accuracy of the DM and minimize the amount of required data input. We began by modelling the system with 6 segments (model UB: 1 wheelchair and lower body, 5 upper body segments). We compared Model UB with the model of a roller-based ergometer (model RL), based on overground propulsion data and a personalized upper body kinematic pattern recorded on a simulator. Then, we simplified model UB to estimate the upper body movement dynamics based on trunk anteroposterior (AP) acceleration (model TR), upper arm AP acceleration (model UA) or forearm AP acceleration (model FA).

Model UB undeniably reduced the RMS velocity prediction error from 0.044 m/s (RL) to 0.026 m/s (UB) and reduced the velocity peak time prediction error from -27.7 % (RL) to 1.7 % (UB). Model UA also reduced the RMS velocity prediction error (0.024 m/s) and velocity peak time prediction error (-7.3 %). Our results suggest that model UA should be used over the RL model in a wheelchair simulator setting for two reasons: 1) it enhances the velocity prediction accuracy; and 2) it requires only one additional data input, i.e., the anteroposterior acceleration of one upper arm. This work has strong implications in the development of future wheelchair simulators that will include upper body movement dynamics without requiring complex real-time motion capture instrumentation.

VI. Acknowledgments

This work was financed by the Natural Sciences and Engineering Research Council of Canada (NSERC), Grants CGSM-424890-2012 and PDF-454531-2014, by the Fonds de recherche du Québec – Nature et technologies (FRQNT), Grant 172173 and by the SensoriMotor Rehabilitation Research Team (SMRRT). The authors want to thank Mathieu Lalumière for his significant contribution with respect to data acquisition. There were no conflicts of interest with this work.

1083-4435 (c) 2015 IEEE. Personal use is permitted, but republication/redistribution requires IEEE permission. See http://www.ieee.org/publications_standards/publications/rights/index.html for more information.

This article has been accepted for publication in a future issue of this journal, but has not been fully edited. Content may change prior to final publication. Citation information: DOI 10.1109/TMECH.2016.2527240, IEEE/ASME Transactions on Mechatronics

ABBREVIATIONS AND SYMBOLS

COM	Centre of mass
RL	Roller ergometer model
d_i	Distance between COM of segment i and proximal articulation (m)
ε_{vel}	Root-mean-square (RMS) velocity prediction error (m/s)
ε_{po}	RMS Power output prediction error (W)
F_{prop}	Propulsive forces (N)
F_{roll}	Rolling resistance (N)
FA	Model based on forearm acceleration
l_i	Length of segment i (m)
M_L	Propulsive moment on the left rear wheel (Nm)
M_R	Propulsive moment on the right rear wheel (Nm)
m	Total mass of the wheelchair/user system (kg)
m_i	Individual mass of segment i (kg)
$m_{\text{participant}}$	Mass of the participant (kg)
Ref. frame 0	Wheelchair origin, located at the middle of the wheelchair's rear wheel axle
r_R	Rear wheels radius (m)
TR	Model based on trunk acceleration
$\ddot{x}_0$	Wheelchair acceleration (m/s^2)
$\hat{\dot{x}}_{0(j)}$	Wheelchair velocity predicted by model j (m/s)
${}^0\ddot{x}_i$	Anteroposterior acceleration of segment i COM relative to ref. frame 0 (m/s^2)
${}^0x_i$	Anteroposterior position of segment i COM relative to ref. frame 0 (m)
$x_{\text{A(L/R)}}$	Anteroposterior position of left/right acromion relative to ref. frame 0 (m)
$x_{\text{E(L/R)}}$	Anteroposterior position of left/right lateral epicondyle relative to ref. frame 0 (m)
$x_{\text{U(L/R)}}$	Anteroposterior position of left/right ulnar styloid relative to ref. frame 0 (m)
x_{XI}	Anteroposterior position of xiphoid process relative to ref. frame 0 (m)
UA	Model based on upper-arm acceleration
UB	Model based on upper-body acceleration

REFERENCES

[1] T. Pithon, T. Weiss, S. Richir, and E. Klinger, "Wheelchair simulators: A review," *Technol Disabil*, vol. 21, no. 1, pp. 1–10, 2009.

[2] M. Blouin, M. Lalumière, D. Gagnon, F. Chénier, and R. Aissaoui, "Characterization of the Immediate Effect of a Training Session on a Manual Wheelchair Simulator With Haptic Biofeedback: Towards More Effective Propulsion," *IEEE Trans Neur Syst Rehabil Eng*, vol. 23, no. 1, pp. 104–105, 2015.

[3] C. Sauret, P. Vaslin, F. Lavaste, N. de Saint Remy, and M. Cid, "Effects of user's actions on rolling resistance and wheelchair stability during handrim wheelchair propulsion in the field," *Med Eng Phys*, vol. 35, no. 3, pp. 289–297, 2013.

[4] C. Sauret, P. Vaslin, M. Dabonneville, and M. Cid, "Drag force mechanical power during an actual propulsion cycle on a manual wheelchair," *Ingénierie et recherche biomédicale (IRBM)*, vol. 30, no. 1, pp. 3–9, 2008.

[5] Y. C. Vanlandewijck, A. J. Spaepen, and R. J. Lysens, "Wheelchair propulsion efficiency: movement pattern adaptations to speed changes," *Med Sci Sports Exerc*, vol. 26, p. 1373, 1994.

[6] F. Chénier, P. Bigras, and R. Aissaoui, "A new wheelchair ergometer designed as an admittance-controlled haptic robot," *IEEE/ASME Trans Mechatronics*, vol. 19, no. 1, pp. 321–328, 2014.

[7] L. R. Crichlow, "Development of a Comprehensive Mathematical Model and Physical Interface for Manual Wheelchair Simulation," Master's thesis, University of Toronto, 2011.

[8] F. Chénier, P. Bigras, and R. Aissaoui, "A new dynamic model of the wheelchair propulsion on straight and curvilinear level-ground paths," *Comput Methods Biomech Biomed Engin*, vol. 18, no. 10, pp. 1031–1043, 2015.

[9] S. S. Rao, E. L. Bontrager, J. K. Gronley, C. J. Newsam, and J. Perry, "Three-dimensional kinematics of wheelchair propulsion," *IEEE Trans Rehabil Eng*, vol. 4, no. 3, pp. 152–160, 1996.

[10] C. P. C. DiGiovine, R. R. A. Cooper, and M. J. Dvornak, "Modeling and analysis of a manual wheelchair coast down protocol," in *Proc of the 19th IEEE-EMBS Annual Conference*, vol. 5, no. C, 1997, pp. 1888–1891.

[11] D. A. Winter, *Biomechanics and Motor Control of Human Movement*, 4th ed. University of Waterloo, Waterloo, Ontario, Canada: John Wiley & Sons, 2009.

[12] M. P. Kadaba, H. K. Ramakrishnan, M. E. Wootten, J. Gainey, G. Gorton, and G. V. B. Cochran, "Repeatability of kinematic, kinetic, and electromyographic data in normal adult gait," *J Orthop Res*, vol. 7, no. 6, pp. 849–860, 1989.

[13] J. Luo, K. Ying, P. He, and J. Bai, "Properties of Savitzky-Golay digital differentiators," *Digital Signal Processing*, vol. 15, no. 2, pp. 122–136, 2005.

[14] R. W. Schafer, "On the frequency-domain properties of Savitzky-Golay filters," in *Proc. 2011 DSP/SPE Workshop*, 2010, pp. 54–59.

[15] S. R. Dubowsky, S. A. Sisto, and N. A. Langrana, "Comparison of kinematics, kinetics, and EMG throughout wheelchair propulsion in able-bodied and persons with paraplegia: an integrative approach," *J Biomech Eng*, vol. 131, no. 2, p. 21015, 2009.

[16] A. M. Koontz, R. A. Cooper, M. L. Boninger, A. L. Souza, and B. T. Fay, "Shoulder kinematics and kinetics during two speeds of wheelchair propulsion." *J Rehabil Res Dev*, vol. 39, no. 6, pp. 635–649, 2002.

[17] M. C. Julien, K. Morgan, C. L. Stephens, J. Standeven, and J. Engsberg, "Trunk and neck kinematics during overground manual wheelchair propulsion in persons with tetraplegia." *Disabil Rehabil Assist Technol*, pp. 1–6, 2013.

[18] C. L. Stephens and J. R. Engsberg, "Comparison of overground and treadmill propulsion patterns of manual wheelchair users with tetraplegia," *Disabil Rehabil Assist Technol*, vol. 5, no. 6, pp. 420–427, 2010.

1083-4435 (c) 2015 IEEE. Personal use is permitted, but republication/redistribution requires IEEE permission. See http://www.ieee.org/publications_standards/publications/rights/index.html for more information.